

Supporting Information

Dopant-Free Hole Transport Material Boosting the Performance of Inverted Methylamine-Free Perovskite Solar Cells

Li Wan, Yulin Tan, Yang Zhao, Lingyun Lou, Zhong-Sheng Wang*

Department of Chemistry, Shanghai Key Laboratory of Molecular Catalysis and Innovative Materials, Laboratory of Advanced Materials, iChEM (Collaborative Innovation Center of Chemistry for Energy Materials), Fudan University, 2205 Songhu Road, Shanghai 200438, China

Experimental Section

Materials

N,N-dimethylformamide (DMF), dichloromethane, petroleum ether, ethyl acetate, toluene, isopropanol (IPA), chloroform and ethanol are obtained from commercial sources and used without further purification. 2,7-dibromo-9H-fluorene, tetrabutylammonium bromide (TBAB), tert-butyl acrylate, [1,1'-Bis(diphenylphosphino)ferrocene]dichloropalladium (Pd(dppf)Cl₂), bis(pinacolato)diboron, distilled DMF, DMSO, chlorobenzene (CB), methanol and 6,6-phenyl C₆₁-butyric acid methyl ester (PCBM) and were purchased from J&K Scientific (China). FAI, PbI₂, CsI, poly[bis(4-phenyl)(2,4,6-trimethylphenyl)amine] (PTAA, M_n ≤ 6000) and bathocuproine (BCP) were purchased from Xi'an Polymer Light Technology Corp (China).

Synthesis Details of PFDTs

(1): 2,7-dibromo-9H-fluorene (3.240 g, 10.0 mmol), TBAB (97 mg, 0.3 mmol) and 30 cm³ distilled toluene were mixed and stirred for 1 h in a three-necked round bottom flask under nitrogen atmosphere. Then, NaOH aqueous solution (2.5 cm³, 50%) was added, and the mixed solution was reacted at 60 °C for 1 h. After 1 h, the tert-butyl acrylate (2.82 g, 22 mmol) was added, and mixed solution was reacted at 60 °C for overnight. Next, water was added to cool the room temperature and the mixture was extracted with dichloromethane. The organic phase was washed with water and dried over Na₂SO₄. The solvent was removed under reduced pressure, and the residue was purified by silica gel column chromatography with petroleum ether and dichloromethane (3:1, v:v) as eluent. **1** was obtained as white solid in 76% yield (4.41 g). ¹H-NMR (400 MHz, CDCl₃, ppm): δ 7.56-7.53 (d, J = 12 Hz, 2H), 7.51-7.49 (d, J = 8 Hz, 4H), 2.34-2.30 (m, 4H), 1.50-1.46 (t, 2H), 1.34 (s, 18H). ¹³C-NMR (100 MHz, CDCl₃, ppm): δ 170.20, 149.96, 139.09, 131.05, 126.48, 122.06, 121.43, 80.45, 54.06, 34.40, 29.84, 28.01.

(2): A mixture of **1** (2.32 g, 4 mmol), potassium acetate (KOAc, 1.57g, 16 mmol) and anhydrous DMF were stirred for 1 h in a three-necked round bottom flask under nitrogen atmosphere. Then, Pd(dppf)Cl₂ (285 mg, 0.4 mmol) and bis(pinacolato)diboron (2.35 g, 8.8 mmol) were added and the mixture was stirred at 80 °C for 12 h. After cooling to room temperature, water was added and the mixture was extracted with chloroform. The organic phase was washed with water and dried over Na₂SO₄. The solvent was removed under reduced pressure, and the residue was purified by silica gel column chromatography with petroleum ether and ethyl acetate (5:1, v:v) as eluent. **2** was obtained as white solid in 68% yield (1.83 g). ¹H-NMR (400 MHz, CDCl₃, ppm): δ 7.85-7.83 (d, *J* = 8 Hz, 2H), 7.80 (s, 4H), 7.74-7.72 (d, *J* = 8 Hz, 2H), 2.42-2.38 (t, 4H), 1.45-1.43 (d, *J* = 8 Hz, 4H), 1.40 (s, 24H), 1.32 (s, 18H). ¹³C-NMR (100 MHz, CDCl₃, ppm): δ 173.08, 148.09, 144.03, 134.57, 129.23, 119.89, 84.11, 80.17, 53.73, 34.67, 30.20, 28.24, 25.16.

(3): In a pre-dried Schlenk tube under nitrogen atmosphere, **2** (405 mg, 0.6 mmol), Pd(dppf)Cl₂ (15 mg, 0.02 mmol), 2,6-dibromospiro[cyclopenta[2,1-b:3,4-b']dithiophene-4,2'-[1,3]dithiolane] (237 mg, 0.6 mmol), K₂CO₃ aqueous solution (2 cm³, 2M) and 15 cm³ distilled toluene were stirred at 100 °C for 48 h. After cooling to room temperature, water was added and the mixture was extracted with chloroform. The organic phase was washed with water and dried over Na₂SO₄. The solvent was removed under reduced pressure and the residue was extracted by a Soxhlet Extractor with methanol, petroleum ether and chloroform sequentially. **3** was obtained as brown solid in 72% yield (306 mg). ¹H-NMR (400 MHz, CDCl₃, ppm): δ 7.84-7.43 (m, 8H), 3.86-3.74 (t, 4H), 2.42-2.40 (d, *J* = 8 Hz, 4H), 1.58 (s, 4H), 1.34 (s, 18H). ¹³C-NMR (100 MHz, CDCl₃, ppm): δ 173.04, 149.85, 134.76, 125.24, 120.79, 119.52, 118.03, 84.15, 80.38, 53.79, 41.85, 34.81, 30.13, 28.26, 25.19.

PFDTs: **3** (200 mg), trifluoroacetate (2 cm³) and distilled chloroform (20 cm³) were mixed and stirred at room temperature for 24 h. Then, the precipitate was obtained by suction filtration and extracted by a Soxhlet Extractor with petroleum ether, acetone and chloroform sequentially. Target product was obtained as brown solid in 60% yield (101 mg). ¹H-NMR (400 MHz, CDCl₃, ppm): δ 11.95 (br, 2H), 7.96-7.73 (m, 6H), 3.39 (s, 4H), 2.87-2.71 (m, 4H), 1.32 (s, 4H). ¹³C-NMR (100 MHz, DMSO) δ 174.35, 149.89, 143.04, 140.23, 136.15, 133.20, 125.68, 120.28, 99.99, 54.19, 29.41. The M_n of PFDTs was determined to be 7.2 kDa, with PDI of 2.2.

Fabrication of Films and Devices

ITO glass ($R_s \leq 15 \Omega$ per square) was cleaned consecutively in detergent, deionized water, acetone, and isopropanol (IPA) ultrasonic baths for 15 min, respectively. Then, ITO glass was treated with UV-Ozone for 20 min. PTAA (2 mg cm⁻³ in CB) and PFDTs (1 mg in methanol by heating and stirring) solutions were spin-coated on the ITO glass at 4000 rpm for 30 s to fabricate a thin hole transport layer (HTL), respectively. Next, the films were annealed at 100 °C for 10 min. Then, a perovskite precursor solution (1.45 M Cs_{0.15}FA_{0.85}PbI₃ in a DMF:DMSO = 3:1, v:v) was deposited on the ITO/HTL substrate

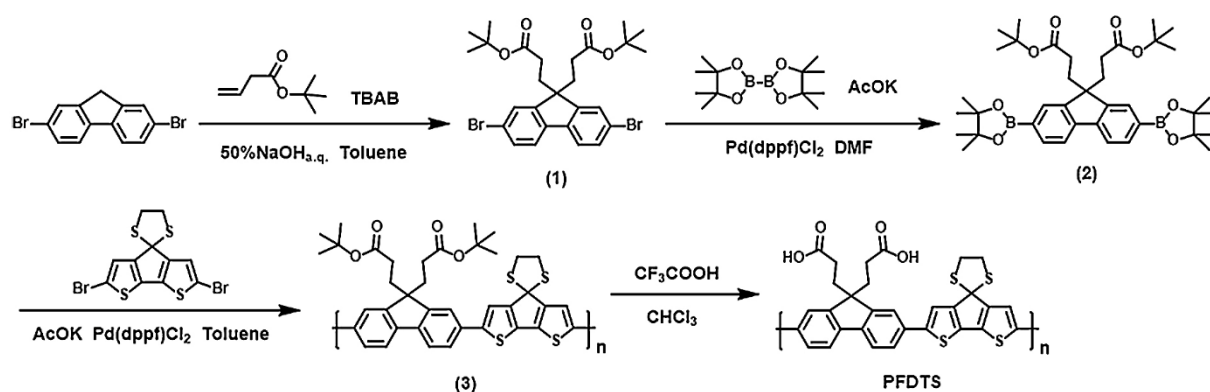
through two step spin-coating at 1000 rpm for 10 s and 5000 rpm for 40 s with CB anti-solvent treatment 20 s before the spin-coating ending. Next, the film was annealed at 60 °C for 1 min and then at 100 °C for 10 min. The PCBM solution (20 mg cm⁻³ in CB) was spin-coated on perovskite film with 2000 rpm for 30 s, next the film was annealed at 100 °C for 5 min. The BCP solution (1 mg cm⁻³ in IPA) was spin-coated with 5000 rpm for 30 s. Finally, 80 nm Ag top electrodes via thermal evaporation (vacuum degree $\leq 2 \times 10^{-4}$ Pa) was deposited. The HTL and perovskite precursor solutions were filtered through a 0.45 μ m polytetrafluoroethylene filter prior to use. The active area is 0.09 cm².

Measurement and Characterization

¹H and ¹³C nuclear magnetic resonance (NMR) spectra were recorded using a 400 MHz Bruker at 293 K using TMS as a reference. Gel permeation chromatography (GPC) was carried out on a ShimadzuSIL-20A liquid chromatography instrument using DMF as eluent at 160 °C with polystyrenes as standards. Cyclic voltammetry (CV) measurements were carried out on a CHI 660e electrochemical analyzer with a three-electrode cell in a deoxygenated anhydrous acetonitrile solution of tetra-n-butylammonium-hexa-fluorophosphate (0.1 M). A platinum disk electrode, platinum-wire, and Ag/AgCl electrode were used as a working electrode, a counter electrode, and a reference electrode, respectively, with the polymer thin film for evaluation coated on the surface of platinum disk electrode. Ferrocene/ferrocenium (Fc/Fc⁺) was used as the external standard (the energy level of Fc/Fc⁺ is -4.8 eV under vacuum). The HOMO energy level was determined from the onset oxidation ($E_{\text{onset}}^{\text{ox}}$) as $\text{HOMO} = -(4.8 + E_{\text{onset}}^{\text{ox}} - E_{\text{onset}}^{\text{Fc}})$ eV, $E_{\text{onset}}^{\text{Fc}}$ equals to the onset oxidation of Ferrocene. Ultraviolet-visible (UV-vis) absorption and reflectance spectra were measured with UV-vis spectrophotometer (Model HP8453). The hole mobilities (μ) were evaluated with the Mott-Gurney law, given by the equation: $J = 9\epsilon_0\epsilon_r\mu V^2 \exp(0.89\beta(V/L)^{1/2})/(8L^3)$, where J stands for the current density, ϵ_0 is the permittivity of free space, ϵ_r is the relative permittivity of the medium, V is the effective voltage, L is the thickness of the active layer and β is the field activation factor.

The density-voltage (J - V) characteristics were recorded with a Keithley 2400 source meter under irradiation of simulated AM 1.5G solar spectrum. The external quantum efficiency (EQE) measurements were conducted with a SM-250 hyper mono-light system (Bunkoukeiki, Japan) combined with a lock-in amplifier and a 150 W Xe lamp in the ambient atmosphere. Ultraviolet photoelectron spectroscopy (UPS) and X-ray photoelectron spectroscopy (XPS) measurements were carried out using a Kratos AXIS ULTRA DALD XPS/UPS system with a He I (21.2 eV) discharge lamp. Fourier transform infrared (FTIR) measurements were performed on Shimadzu IRAffinity-1 FTIR spectrometer. The scanning electron microscopy (SEM) of devices were observed by SEM system (S4800, Hitachi, Japan). The atomic force microscopy (AFM) images were observed on a Dimension 3100 V AFM (Veeco, USA, tapping mode). The thicknesses of each layer were monitored upon deposition by using a crystal thickness monitor (Sycon). Photoluminescence (PL) and Time-resolved photoluminescence (TRPL) spectra

were analyzed using a fluorescence spectrophotometer (RF-5301PC, Shimadzu) with a 150 W Xe lamp as the excitation source at room temperature, and the excitation wavelength was 520 nm. TRPL curves were fitted by the bi-exponential function, and the function formulas are $y = A_1 \times \exp(-t/\tau_1) + A_2 \times \exp(-t/\tau_2)$ and $\tau_{ave} = A_1 \times \tau_1 + A_2 \times \tau_2$, where τ_1 is the fast decay lifetime, τ_2 is the slow decay lifetime, τ_{ave} is the average lifetime, A_1 and A_2 are the corresponding proportion, respectively. The crystallinity of the as-prepared samples was analyzed using a powder X-ray diffractometer (XRD, Bruker AXS D8 Advance, Germany) equipped with a Cu K α radiation source ($\lambda = 0.154$ nm). The formula for calculating the trap density of the space-charge-limited current (SCLC) model is $N_t = 2\epsilon\epsilon_0 V_{TFL}/(qL^2)$, where q is the elementary charge of the electron, L is the perovskite film thickness, and ϵ and ϵ_0 are the relative dielectric constant and the vacuum permittivity. The formula for calculating V_{OC} as a function of light intensity (I) is $V_{OC} = nKT \ln(I)/q$, where n is ideal factor, K is the Boltzmann constant, T is absolute temperature, and q is the electron charge. The electrochemical impedance spectroscopy (EIS) measurement was carried out under dark at a reverse potential of 0.8 V at frequencies ranging from 1.0 Hz to 1.0 MHz and the oscillation potential amplitudes are 20 mV using the Zahner IM6 system.



Scheme S1. The synthesis details of PFDTs.

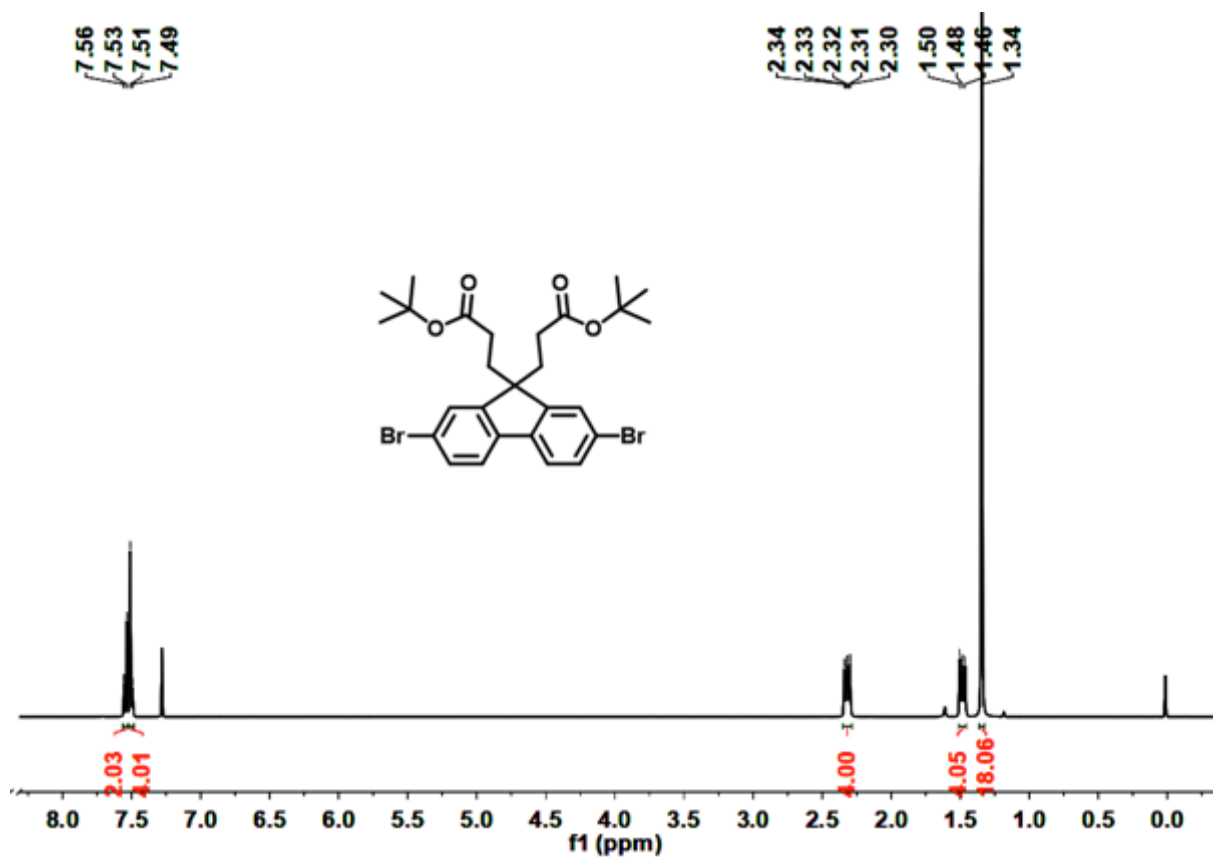


Fig. S1. The ^1H NMR spectrum of 1.

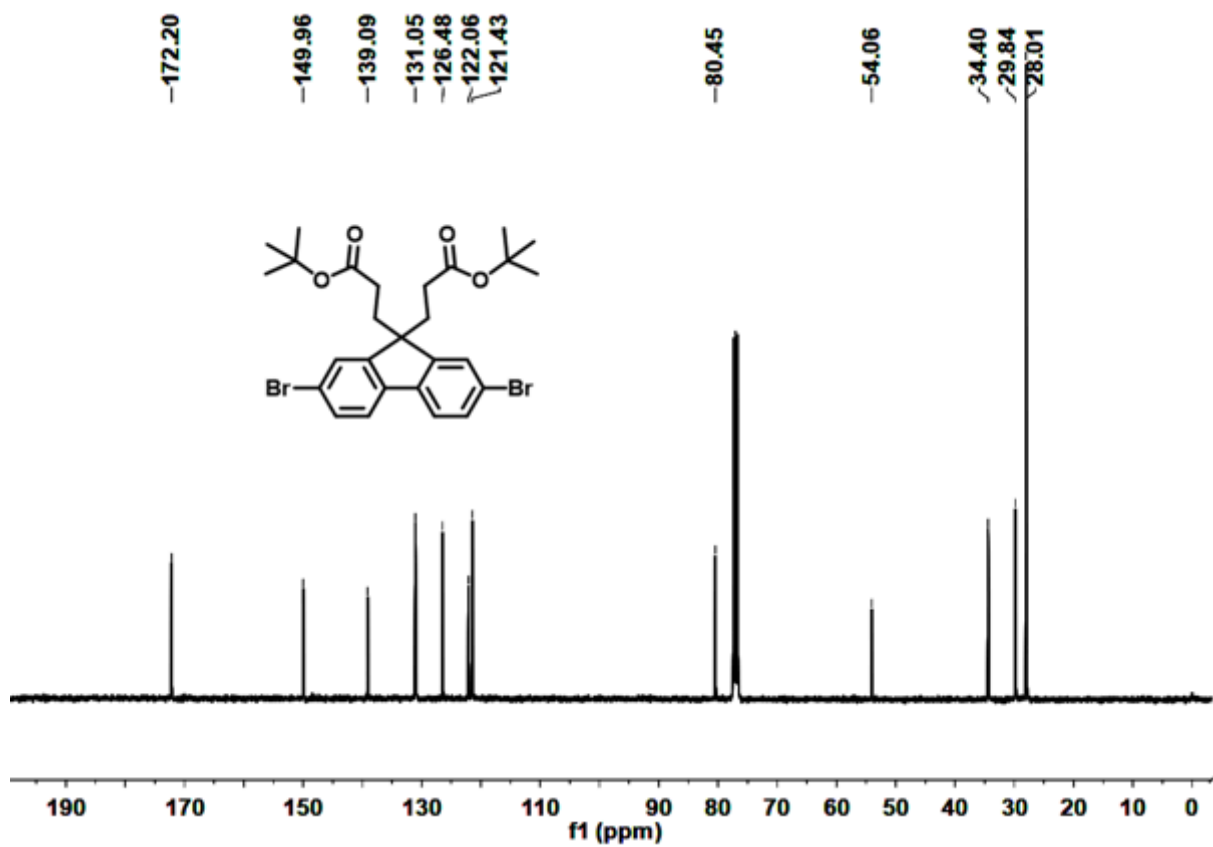


Fig. S2. The ^{13}C NMR spectrum of 1.

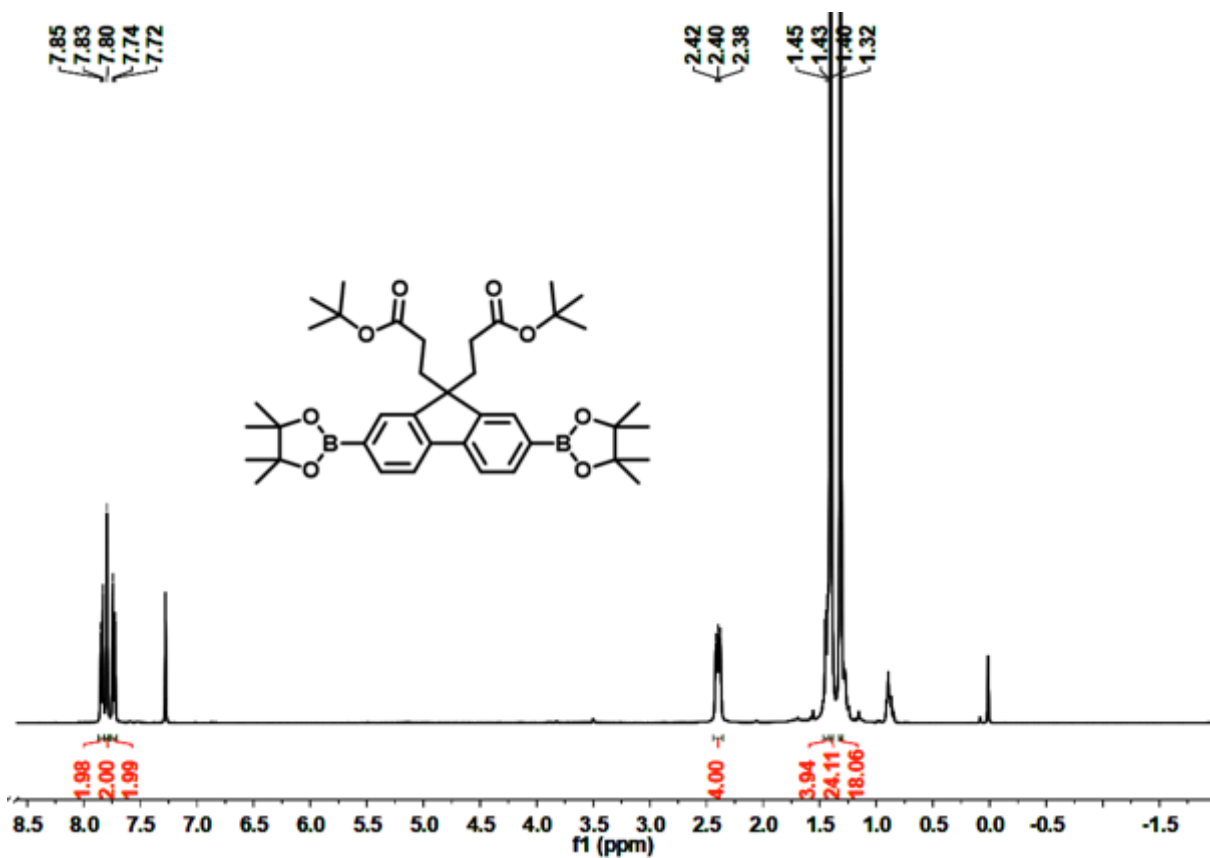


Fig. S3. The ¹H NMR spectrum of 2.

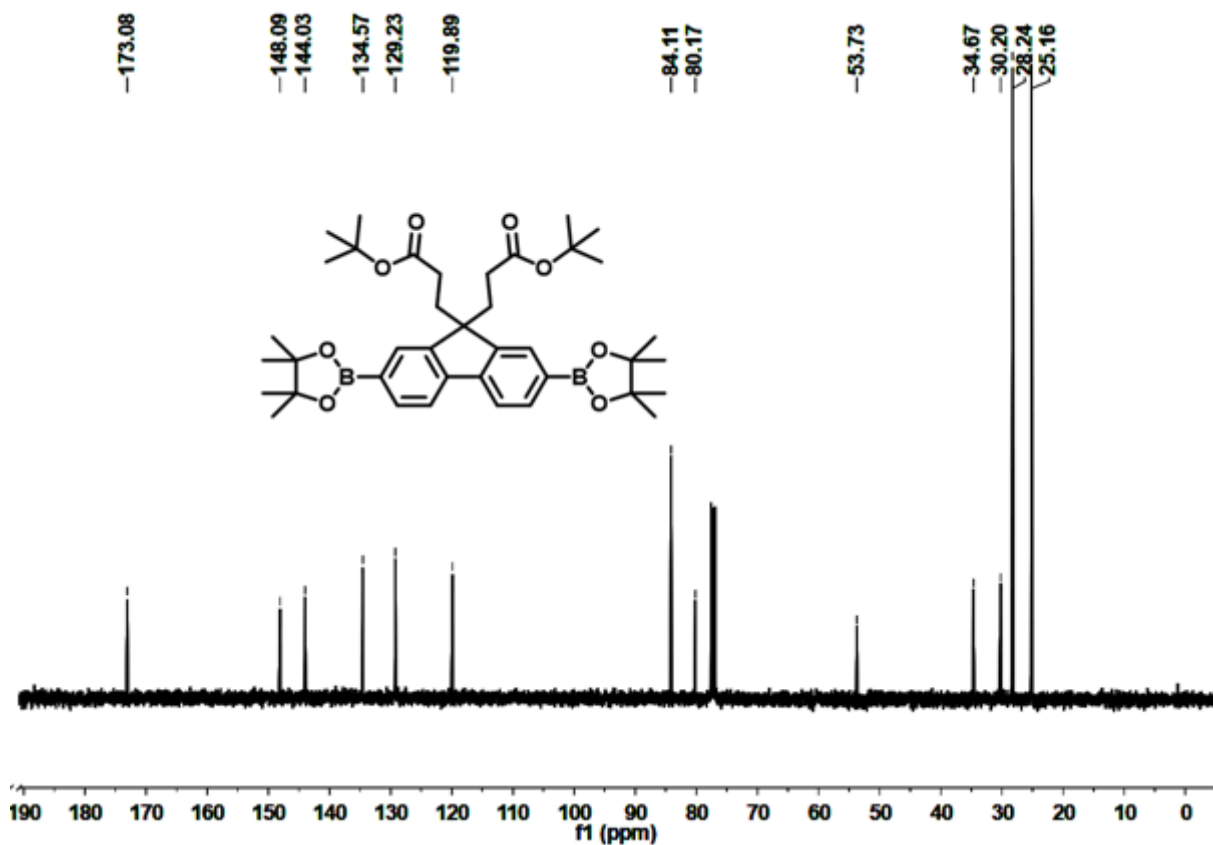


Fig. S4. The ¹³C NMR spectrum of 2.

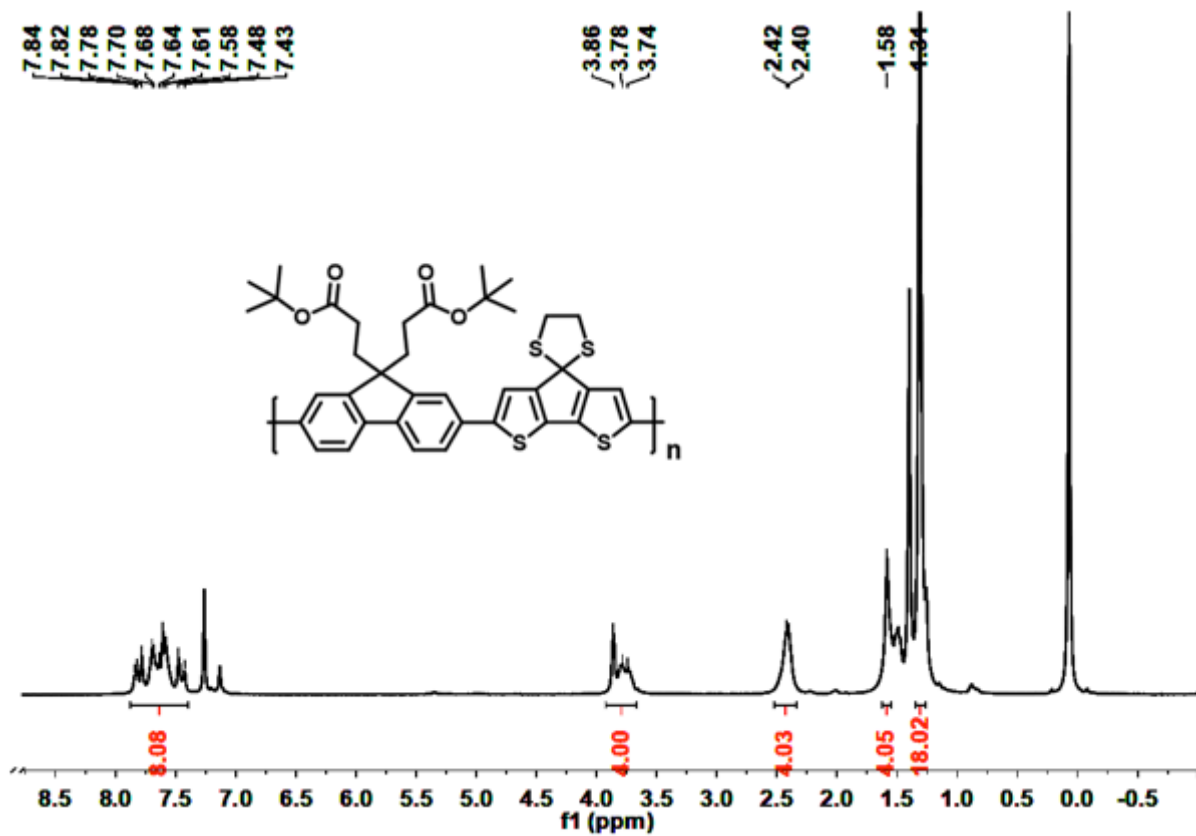


Fig. S5. The ^1H NMR spectrum of 3.

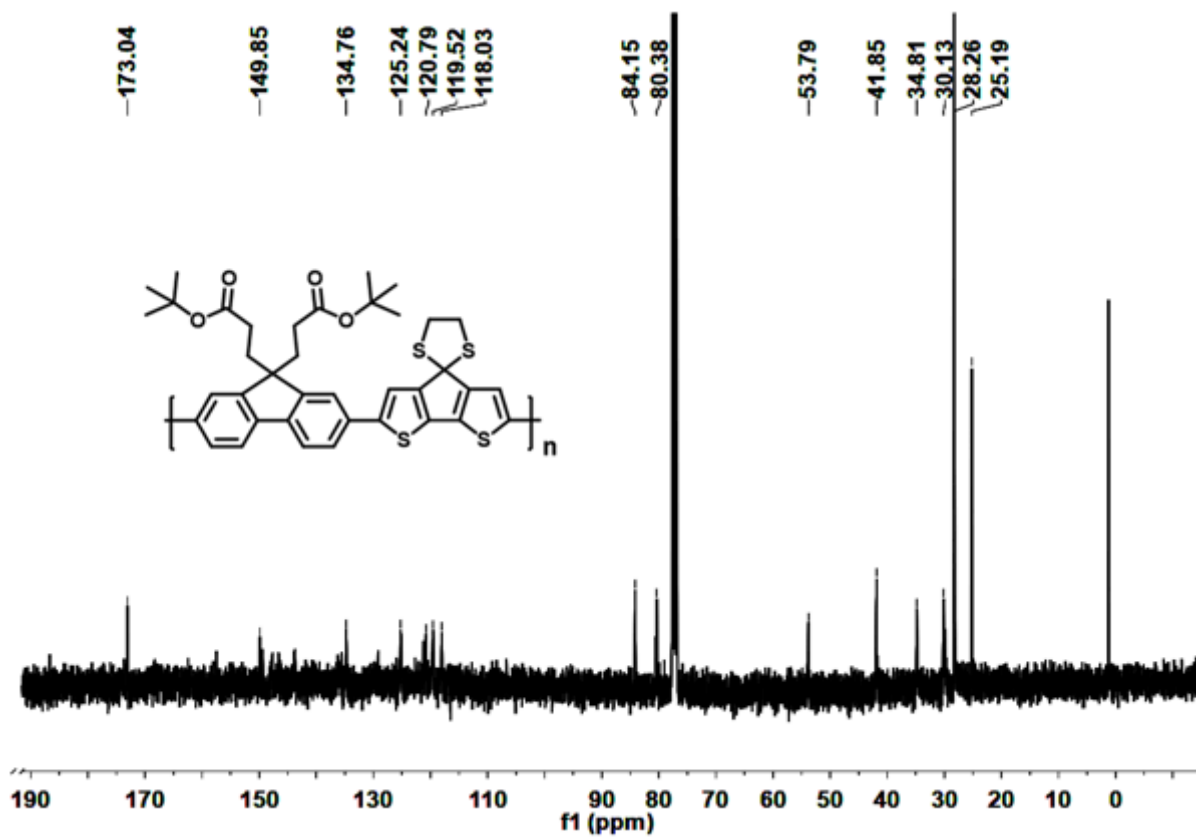


Fig. S6. The ^{13}C NMR spectrum of 3.

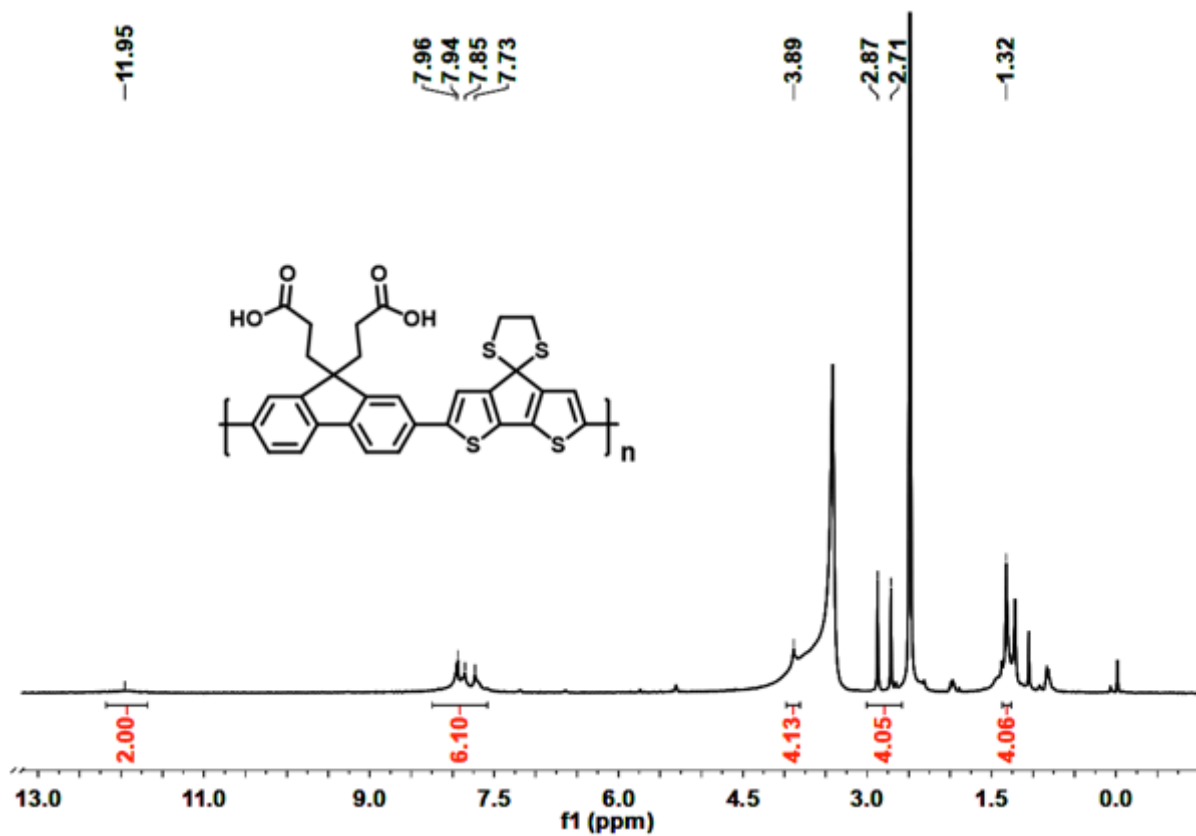


Fig. S7. The ¹H NMR spectrum of PFDTs.

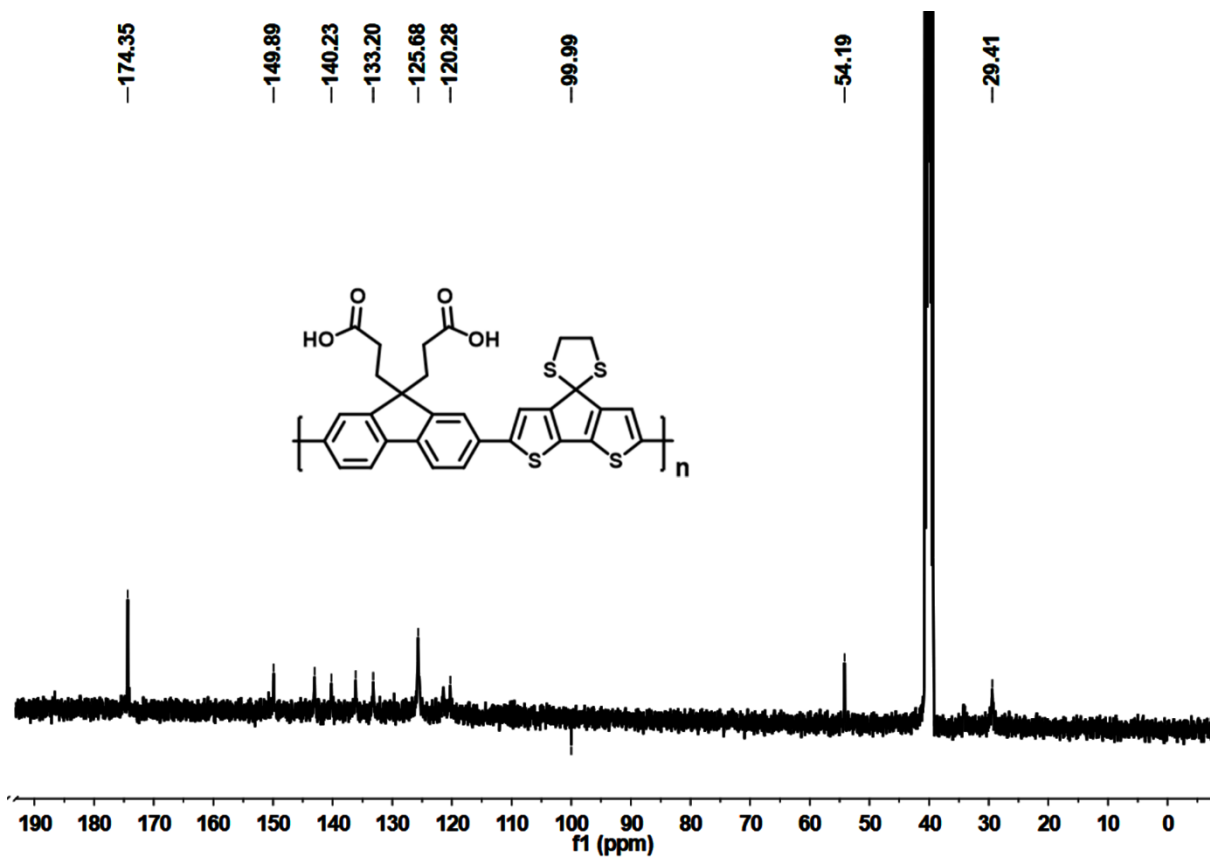


Fig. S8. The ¹³C NMR spectrum of PFDTs.

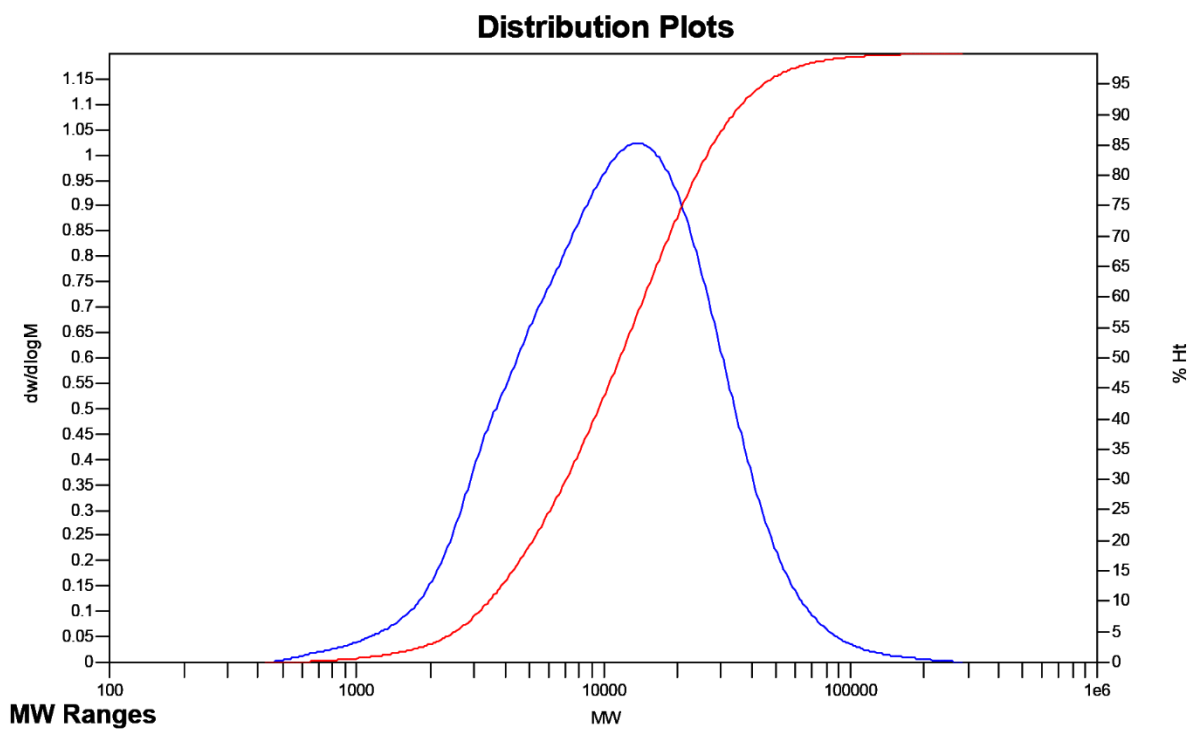


Fig. S9. The GPC curves of PFDTs.

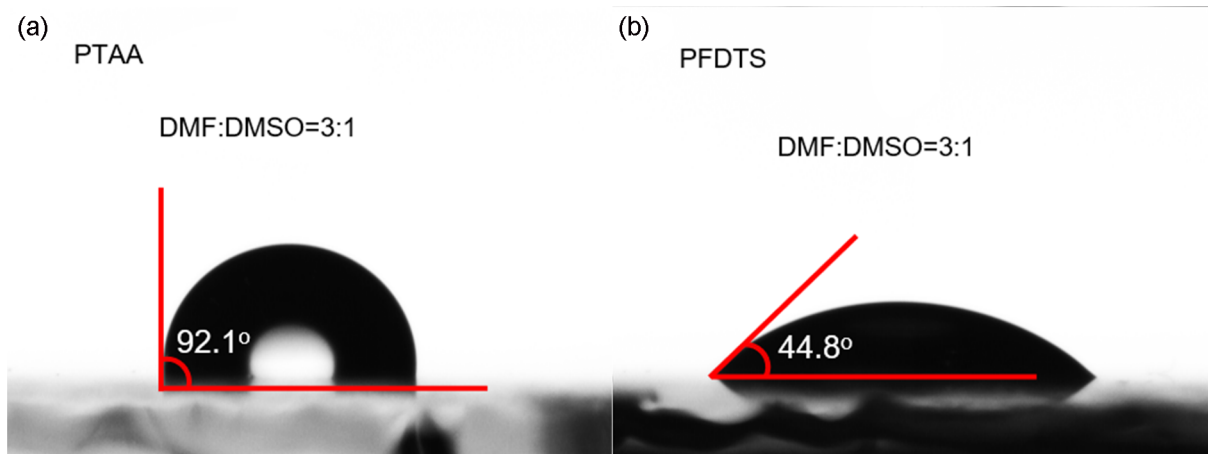


Fig. S10. Contact angle of a mixture solvent (DMF:DMSO = 3:1, v:v) on (a) the PTAA film and (b) the PFDTs film, respectively.

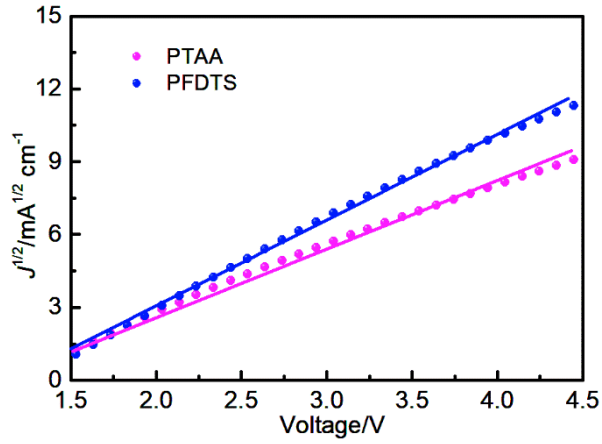


Fig. S11. Hole mobility curves of PTAA and PFDTs using the SCLC model.

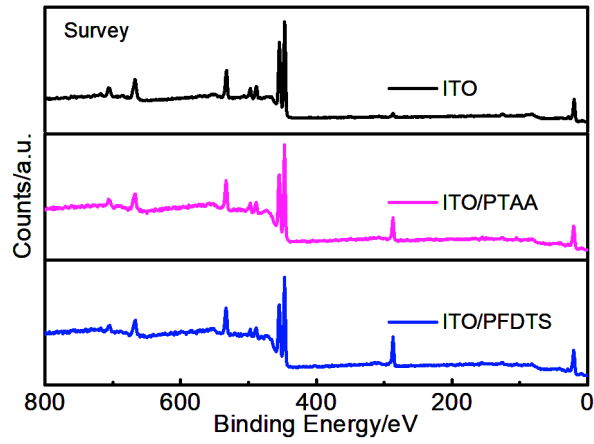


Fig. S12. Survey XPS of ITO, ITO/PTAA and ITO/PFDTs.

Table S1. Parameters of the TRPL spectra of perovskite films with different HTL (τ_1 and τ_2 represent the time constant of the two decay processes, τ_{ave} is the average carrier lifetime).

Sample	τ_1 /ns	A_1 /%	τ_2 /ns	A_2 /%	τ_{ave} /ns
Perovskite	177.7	32.8	465.8	67.2	371.1
PTAA/Perovskite	96.1	41.3	232.6	58.7	176.2
PFDTs/Perovskite	39.6	52.5	83.1	47.5	60.3

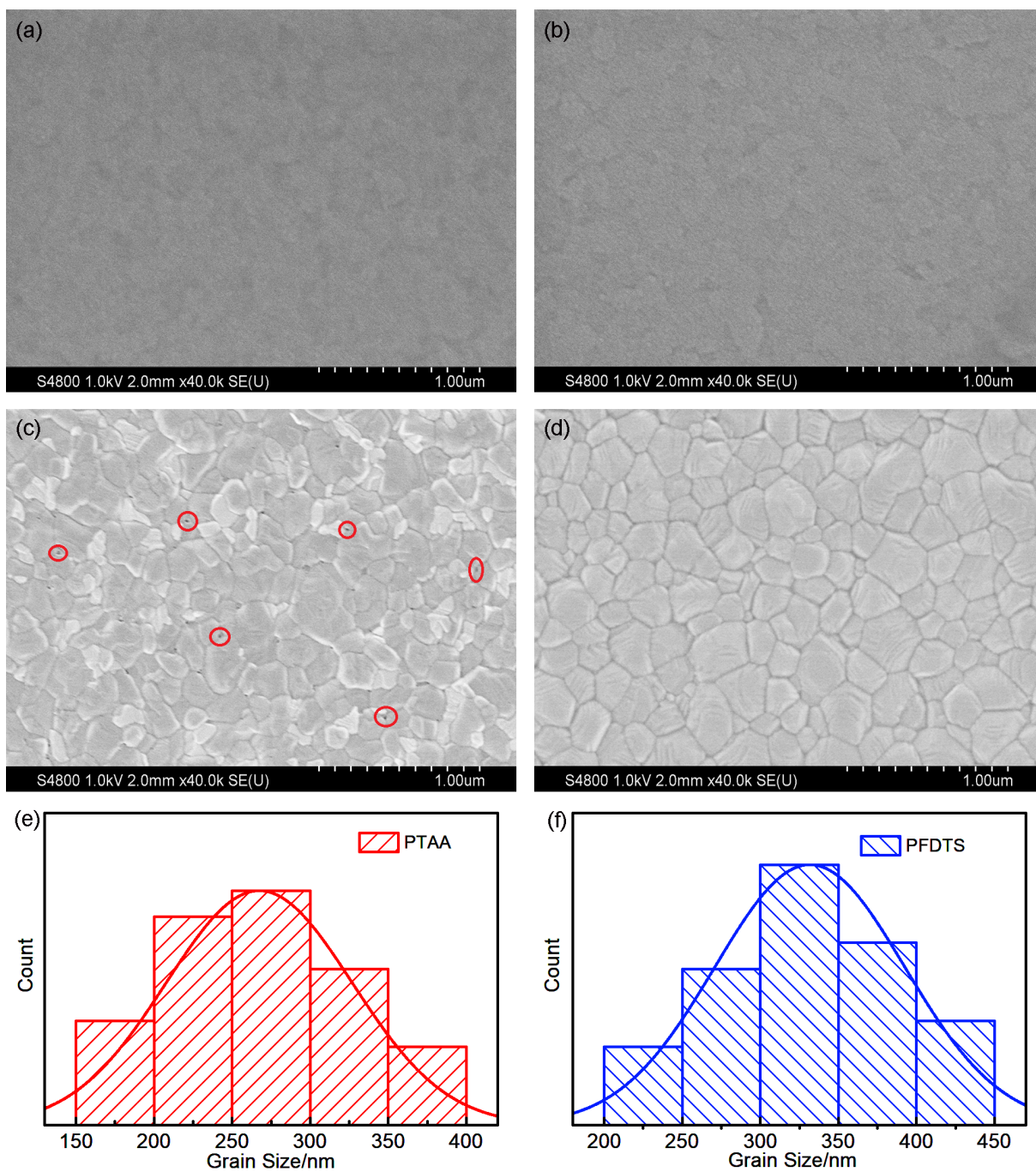


Fig. S13. The SEM images of (a) PTAA film, (b) PFDTS film, (c) PTAA/Perovskite film, and (d) PFDTS/Perovskite film. Diagrams of perovskite grain sizes based on different HTL: (e) PTAA and (f) PFDTS.

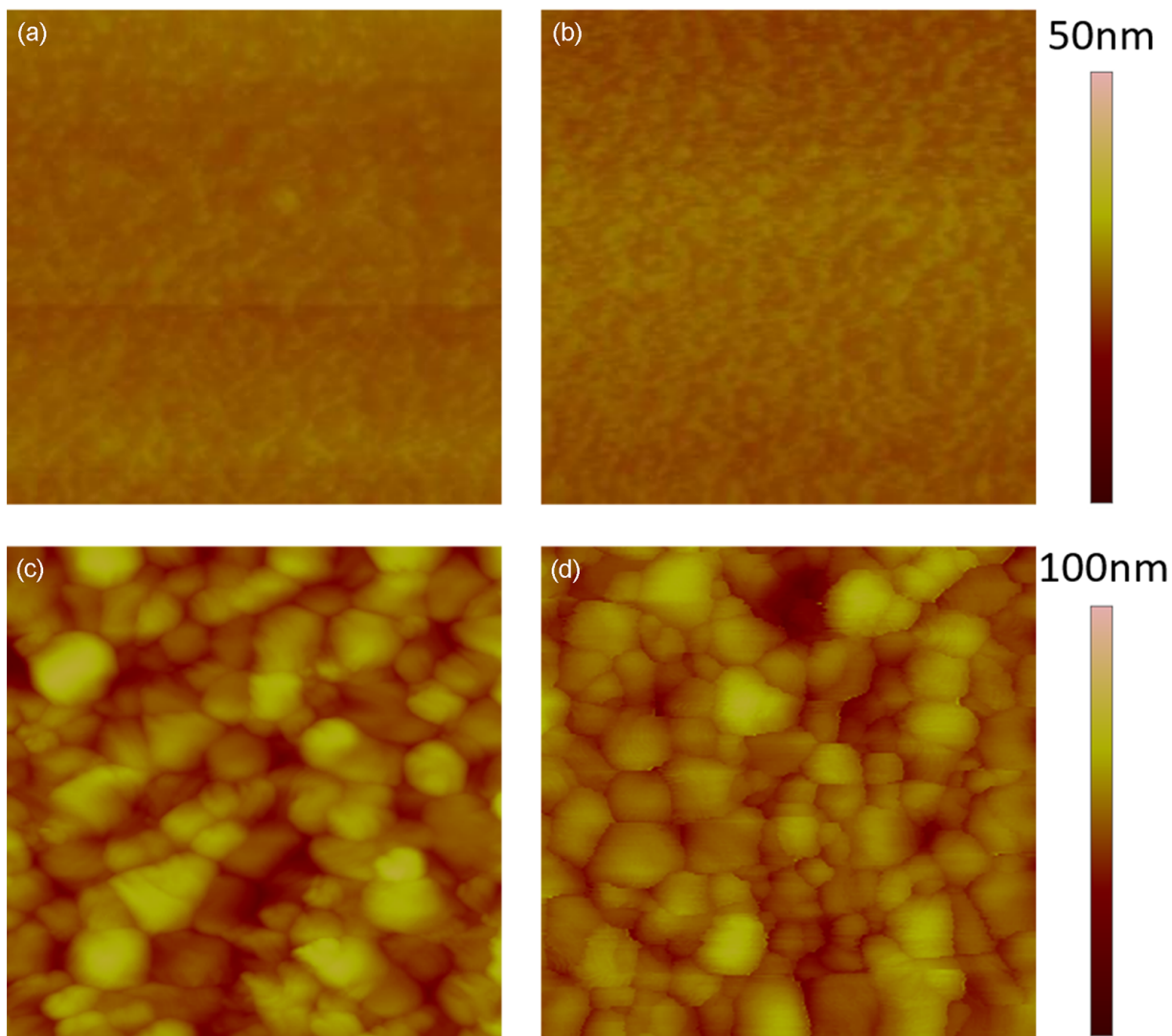


Fig. S14. The AFM images ($3 \mu\text{m} \times 3 \mu\text{m}$) of (a) PTAA film, (b) PFDTs film, (c) PTAA/Perovskite film, and (d) PFDTs/Perovskite film.

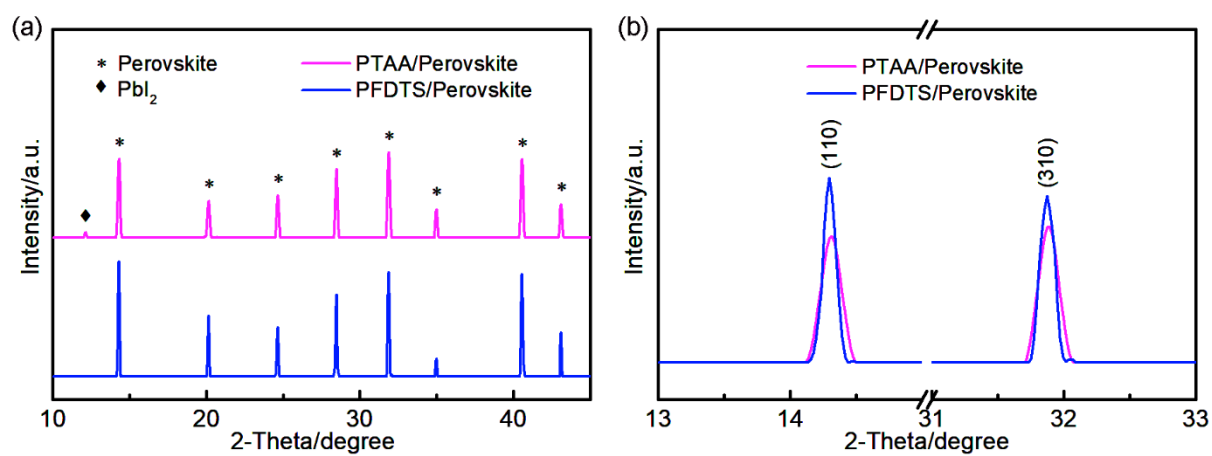


Fig. S15. (a) XRD spectra of PTAA/Perovskite and PFDTs/Perovskite. (b) Magnified view of crystal planes of (110) and (310).

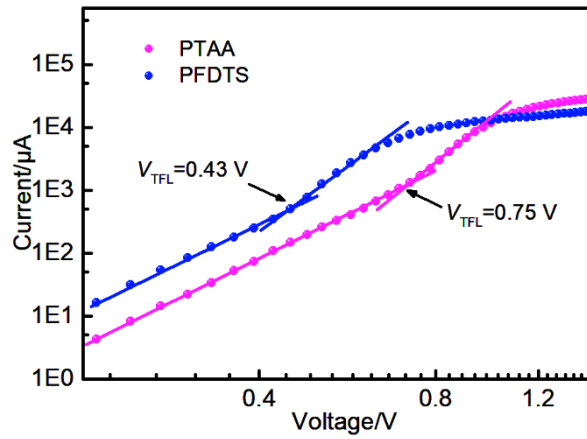


Fig. S16. SCLC curves of ITO/HTL(PTAA or PFDTs)/perovskite/Spiro-OMeTAD/Ag.

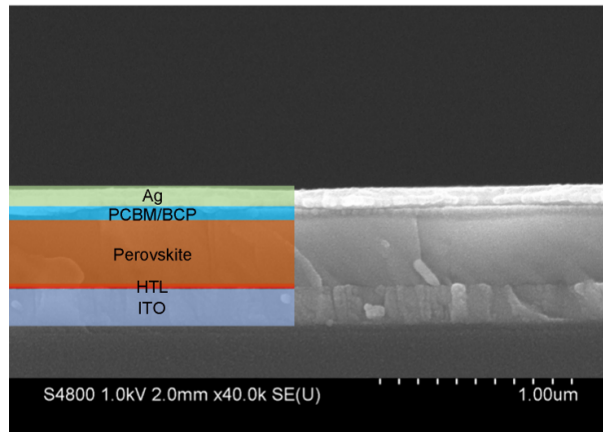


Fig. S17. The cross-section image of a complete PSC device.

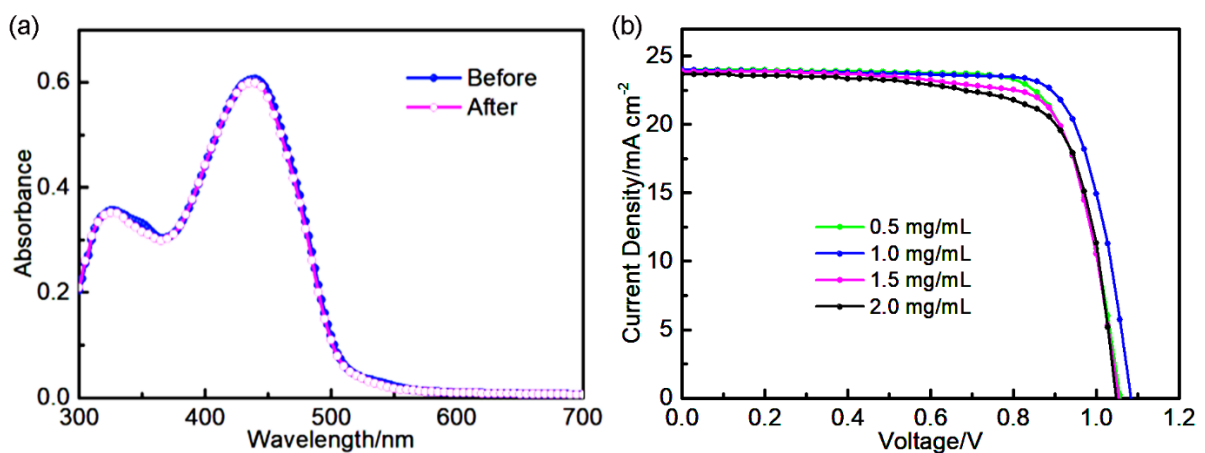


Fig. S18. (a) UV-vis absorption spectra of the PFDTs film and that after spin coated with the perovskite precursor solvent. (b) The J - V curves of PSCs fabricated with different concentrations of PFDTs.

Table S2. Photovoltaic parameters of devices based on PFDTs with different concentrations.

Concentrations/mg cm ⁻³	V_{oc}/V	$J_{sc}/mA\text{ cm}^{-2}$	FF/%	PCE/%
0.5	1.057	23.99	75.5	19.14
1.0	1.082	24.03	77.5	20.15
1.5	1.054	23.86	75.3	18.94
2.0	1.048	23.74	73.2	18.22

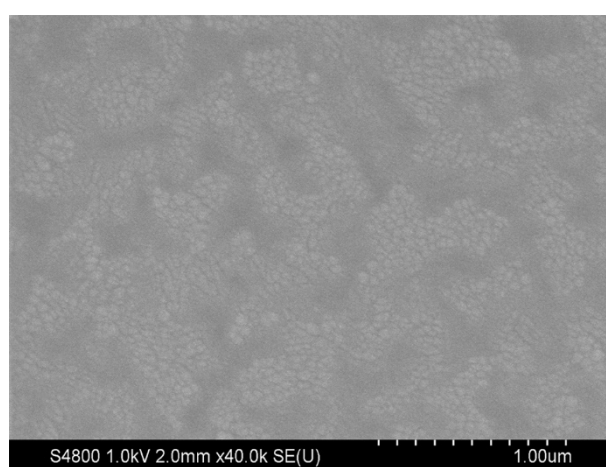


Fig. S19. The top-view SEM image of the PFDTs film fabricated at low concentration.

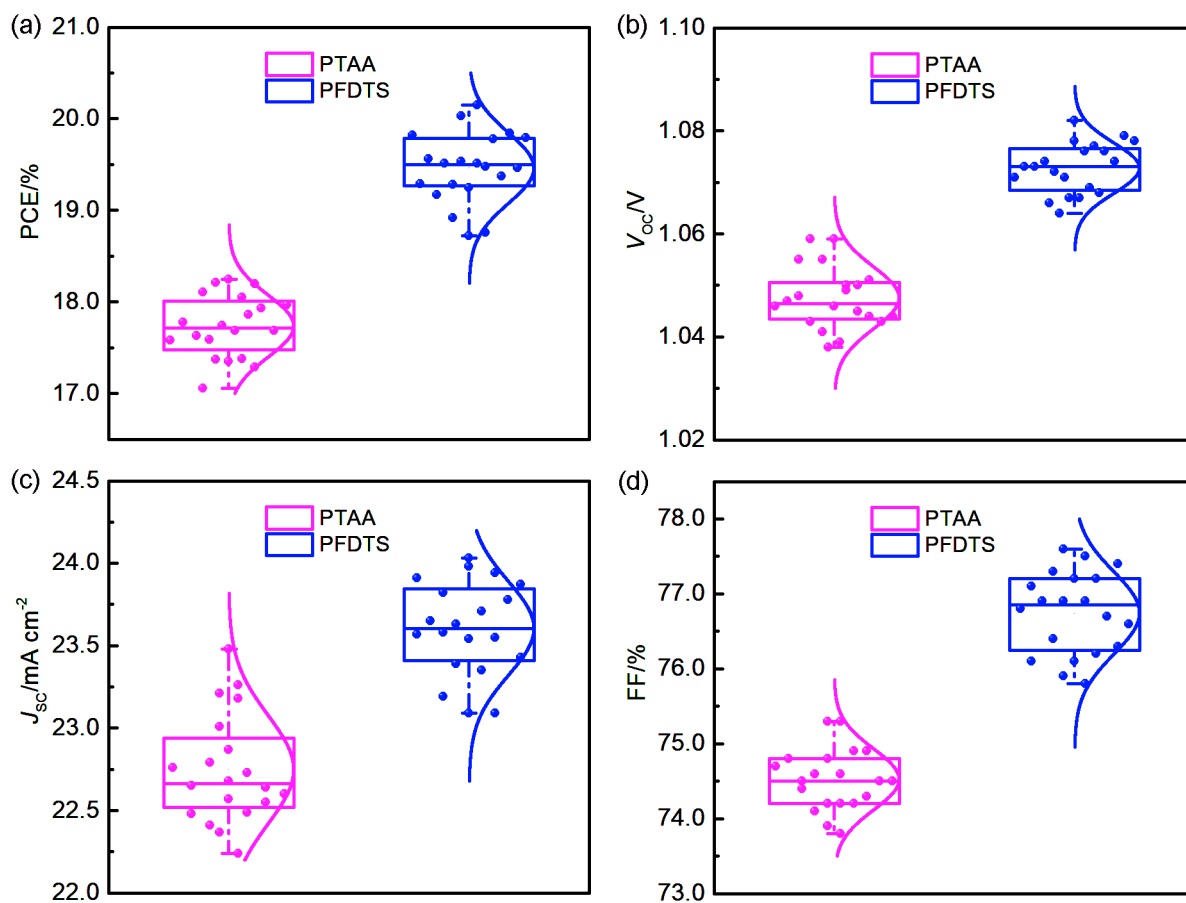


Fig. S20. Diagrams of (a) PCE, (b) V_{oc} , (c) J_{sc} and (d) FF measured from 20 devices.

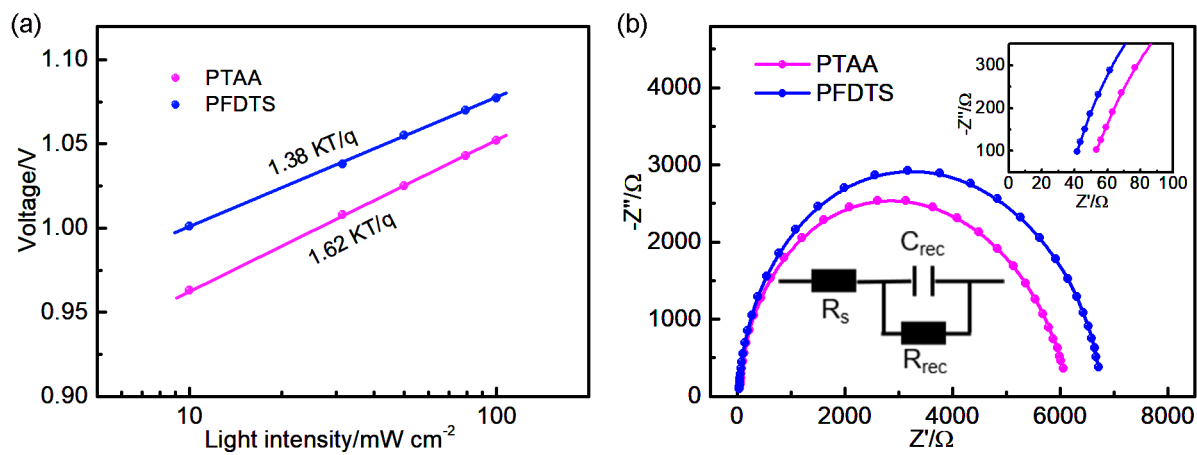


Fig. S21. (a) The V_{oc} of different devices as a function of light intensity. (b) EIS Nyquist curves, in which the magnified curve at the high-frequency region and the equivalent circuit are inserted.